141
9-24-80

Dr. 1791

LA-8490-PR

Progress Report

MASTER

NDA Technology for Uranium Resource Evaluation

July 1—December 31, 1979

University of California

LOS ALAMOS SCIENTIFIC LABORATORY
Post Office Box 1663 Los Alamos, New Mexico 87545

LA-8490-PR
Progress Report
UC-51
Issued: August 1980

NDA Technology for Uranium Resource Evaluation

July 1—December 31, 1979

Compiled by

M. L. Evans

CONTENTS

NDA TECHNOLOGY FOR URANIUM RESOURCE EVALUATION

July 1, 1979--December 31, 1979

Compiled by

M. L. Evans

ABSTRACT

This report describes work performed during the time period from July 1, 1979, to December 31, 1979, on the contract for Nondestructive Nuclear Analysis (NDA) Technology for Uranium Resource Evaluation in Group Q-1. Calculational effort was focused on improving the accuracy with which detector response function maps can be generated for subsequent enfolding with ONETRAN angular flux data. Experimental effort was highlighted by a field test of the prototype photoneutron logging probe at the Grand Junction DOE calibration facility. The probe demonstrated adequate durability in the field and sufficient sensitivity to uranium to function at competitive logging speeds.

I. GAMMA-RAY SPECTRAL CALCULATIONS

(M. L. Evans)

A major goal of the spectral calculations is to provide theoretical pulse-height spectra observed in gamma-ray detectors used in potassium, uranium, and thorium (KUT) spectral logging. Theoretically determined window sensitivities and stripping ratios will prove invaluable in defining the usefulness and applicability of the KUT method to the many different logging geometries and environments. However, the utility of the calculated spectra depends critically on their accuracy and precision. A target of 10% has been chosen as the maximum tolerable uncertainty (i.e., including both sytematic and statistical errors) in the theoretical pulse-height spectra. This value is comparable to that obtainable with carefully controlled physical borehole models.

Pulse-height spectra calculated by enfolding detector response functions with ONETRAN angular flux spectra are subject to several sources of error. The uranium and thorium spectral line intensities input to ONETRAN are generally known to only about 3-5%. The uncertainties in the angular flux values computed using discrete ordinates methods depend on many factors including the photon energy, spacing of mesh points, Legendre order of the cross-section expansion, and the angular quadrature order, to name the most important. For the simple geometries of the airborne and subsurface ONETRAN models, the angular fluxes are probably accurate to about 2% for photon energies higher than 100 keV. At energies below 100 keV, computer core memory requirements preclude a sufficient number of spatial mesh points being included in the ONETRAN models to ensure accurate calculation of the fluxes. Uncertainties arising from approximations assumed in the enfolding process probably contribute no more than about 2% error in the resulting pulse-height spectra for the airborne and subsurface geometries. Thus, added linearly, the total uncertainty in the pulse-height spectra is probably 7-9% neglecting contributions from the detector response function. In reality, the various components of error most likely do not add

linearly, but instead, partially cancel one another in the spatial and angular averaging of the enfolding process (more will be said about this later). Therefore, a more realistic estimate of the error excluding those of the response function is probably 5-6%. Thus, to satisfy the 10% upper limit on the errors in the computed pulse-height spectra, the detector response function needs to be determined to about 5% accuracy. The statistical imprecision of the response function is not an issue here, since it can be reduced to negligible levels (≈1%) for any spectral region of interest, without requiring unduly long computing time, owing to the high execution speed of the GAMRES code.

The systematic uncertainty in the pulse-height distributions computed using GAMRES is primarily due to errors in the photon cross-section parameterizations. The magnitude of these errors depends on both the material and photon energy but generally contributes about 2-3% uncertainty to the absolute determination of the pulse-height distributions. Approximations employed in simulating photon transport add another per cent or more to the spectral uncertainty, especially at high energies, because electron energy losses resulting from bremsstrahlung escape are estimated only to first order. Thus, the systematic error in the pulse-height distributions are probably on the level of 3-4%.

An uncertainty of 3-4% in the single-energy pulse-height distributions computed by GAMRES results in an upper limit of about 1% in the uncertainty allowed the response function mapping technique. The scheme originally proposed for mapping[1] the response function used a two-dimensional spline interpolation technique to yield an analytically continuous representation of the energy vs pulse-height surface from a coarse map produced by running GAMRES at widely spaced photon energies. The scheme had the advantage that the resulting response function was continuous and thus could be evaluated at any arbitrary values of energy and pulse height. This general purpose map would be independent of the energy group structure of the ONETRAN angular fluxes with which it would be enfolded, and it would yield pulse-height spectra with any given pulse-height binning structure. However, results indicate that interpolation errors (especially in the energy direction) could be reduced within 1% only by the use of relatively closely spaced single-energy pulse-height distributions in the basic map produced by GAMRES. In addition, the techniques used to check the resulting energy vs pulse-height surfaces were difficult and time consuming in their application.

An alternate scheme is now being used to produce accurate response function maps. Instead of generating a map that is of general use, a high-precision map is computed for a specific application. In the mapping procedure, the energy regions of the map that are especially important to the specific application are determined with greater precision than those regions that are less important. That is, GAMRES is set up to run more photon histories for the energies of interest and to neglect other regions of the map. In this way, most of the computing time spent on generating the map is used to yield high-precision response functions for the energies of interest. The map is made even more specific to the application, because not only are the mapping energies chosen specifically for the given application but the binning of the map in the pulse-height direction is also specified at the time of map generation. The resulting map is no longer of general use, but it is both more precise in the energy regions of interest and more accurate than a general map because no interpolation of the energy vs pulse-height surface is required. Thus, the accuracy of the application-specific map is that of the GAMRES code, about 3-4% over the photon energy range 0-3 MeV.

Detector response function maps have been computed for right cylindrical NaI crystals of various diameters and heights. A mapping verion of the GAMRES code was set up to produce a map containing 265 pulse-height distributions, one for each group of the 265-group structure used in ONETRAN for the airborne and subsurface flux calculations. Thus, the photon energies chosen for mapping were those corresponding to the centers of the energy bins used in ONETRAN, that is, 15 keV, 25 keV, ..., 2.615 MeV. All pulse-height distributions were binned in 300 10-keV-wide channels with the first channel containing events with pulse heights from 0-10 keV and the last channel spanning the range from 2.99-3.00 MeV.

The maps were designed for use in computing estimates of window sensitivies and stripping ratios for KUT airborne and surface logging applications. Thus, the number of photon histories run at each of the 265 map energies were chosen to yield enfolded pulse-height spectra that would provide high-precision count-rate estimates in the K, U, and Th windows. This was accomplished by using the following weighting algorithm that strongly favors the K, U, and Th lines in the KUT region, that is, from about 1-3 MeV. For mapping energies in the KUT region that correspond to flux groups containing source lines (from K, or U, or Th), the number of photon histories run at that energy is proportional to the intensity of the source line on the basis of photons emitted per second per gram of parent material. The number of photon histories run at mapping energies in the KUT region not corresponding to source lines was chosen to be a small constant value, since the detector response attributable to these flux groups would be small compared with that from the groups containing source lines. At energies below 1 MeV (outside the KUT region), the number of histories run at a given energy was proportional to the energy. That is, higher energy responses were determined with greater precision. This scheme was used because the low-energy responses are of less importance in both gross gamma and spectral gamma logging, and because the precision of enfolded spectra is good in this region because of the fact that all higher energy responses contribute events to the lower pulse-height channels.

The weighting algorithm for mapping detector response functons described above has been used to generate energy versus pulse-height maps for NaI detectors having various dimensions. Twenty minutes of CDC 7600 computer time will generally result in a map of sufficient precision to yield KUT window sensitivity values with statistical uncertainties less than about 0.5%. This mapping procedure will be used for all subsequent detector response function determinations.

II. TEST AND EVALUATION OF THE FIELD PROTOTYPE PHOTONEUTRON-BASED LOGGING PROBE

(M. P. Baker, T. Marks, R. Kuoppala, and T. Dye)

A. Introduction

The fabrication of the field prototype photoneutron-based logging probe for direct uranium ore-grade determination was recently completed at LASL.[2] The performance of the probe was evaluated at the Grand Junction DOE calibration facility in collaboration with Bendix Field Engineering Corporation (BFEC) personnel. LASL provided the photoneutron-based probe including uphole pulse-processing and control electronics; BFEC supplied a logging vehicle (CFMS) equipped with an ND660 computer-based multichannel analyzer and peripherals.

Static and dynamic uranium logs were obtained in the A and D models over a period of about 10 days. There were no probe failures of any kind. However, the probe housing was opened to exchange detectors for additional water factor measurements. The probe again functioned properly following the reassembly. The data obtained at Grand Junction served to calibrate the probe, determine the effects of borehole diameter and fluid, and assess the impact of certain formation parameter changes.

A brief review of the physics of the photoneutron-based logging techniques will be given, the probe and associated components will be described, the data obtained at the calibration facility will be presented, and the conclusions that can be drawn will be discussed.

B. Principles of the Photoneutron-Based Method

The photoneutron-based logging system uses high-energy gamma rays from an 10-Ci ^{124}Sb source to produce low-energy neutrons via the (γ,n) reaction in a beryllium assembly (see Fig. 1). These low-energy neutrons diffuse into the formation being logged and produce fissions in the uranium present. Only the ^{235}U nuclei (0.72% by weight) undergo fission because the interrogating photoneutrons are lower in energy (24 and 400 keV) than the fission threshold of ^{238}U. The fission of a ^{235}U nucleus results in the prompt emission of two 2-MeV neutrons on average.

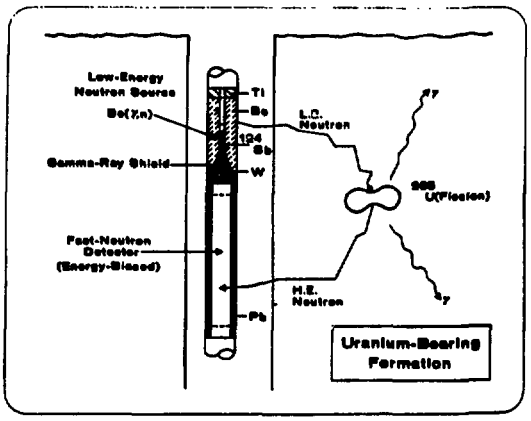

Fig. 1. Schematic representation of photoneutron-based well-logging probe components, the fission process, and detection of fission neutrons in a uranium-bearing formation.

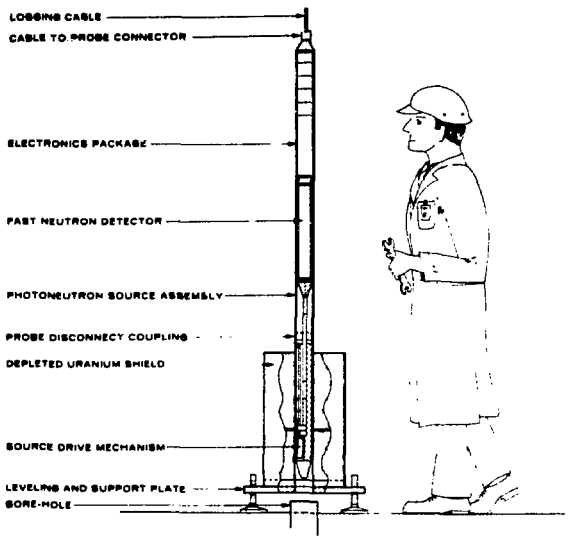

Fig. 2. Photoneutron-based uranium well-logging probe in use in the field.

Some of these high-energy, fission neutrons that are emitted return to the borehole probe where they are detected by an 18-atm helium recoil proportional counter biased to prevent the counting of the lower energy source neutrons. Thus, the system is operative 100% of the time, and no source pulsing or modulation is required.

C. Photoneutron-Based Logging System

The LASL logging system consists of the 6.7-cm (2-5/8-in.) diam by 2.3-m (7-1/2-ft) long logging probe, transportation cask, leveling and support plate, and uphole electronics control module. The logging winch, its controller, and the ND660 computer-based multichannel analyzer with its peripherals were provided by EPEC. Figure 2 illustrates how the probe is used in the field.

The lower section of the probe, containing the ^{124}Sb gamma-ray source, is stored in a depleted uranium container, which serves as a biological shield during transportation and during use at the logging site. The upper section of the probe, containing all the remaining components, is stored on the logging vehicle. In preparation for logging, the leveling and support plate and source container are positioned over the borehole, and the upper probe section is connected to the logging cable. With the lid of the source container removed, the top section of the probe is lowered with the winch onto the bottom section retained in the source container. The two probe sections are fastened together with a coupling ring. The assembled probe is lifted slightly with the winch to allow a trap door at the bottom of the source container to be opened. This allows the probe to be lowered through the shield and into the borehole.

A small motor at the bottom of the probe permits the photoneutron source to be turned on and off remotely. This is achieved by driving the ^{124}Sb source capsule between a tungsten-shielded position in the lower section of the probe and a beryllium sleeve in the upper probe section. Thus, there are no neutrons produced until the probe has been lowered into the borehole. The gamma-ray source position is monitored by a pair of microswitches in the lower probe section whose state is communicated to the uphole control electronics. In addition, a microswitch on the cask determines whether the probe is deep within the borehole or approaching the surface. If an attempt is made to remove the probe from the borehole without withdrawing the gamma-ray source from the beryllium, an alarm is sounded.

The source-detector section of the probe consists of a beryllium converter for photoneutron production and conical and cylindrical, tungsten shadow shields for the 18-atm helium recoil proportional counter. The 5.1-cm (2-in.)-diam by 30.5-cm (12-in.)-active length detector is cadmium wrapped

to reduce the background produced by thermal neutron captures in the small (1.4×10^{-6}), natural abundance of ^3He in normal helium.

Three P.C. boards make up the electronics package that occupies the topmost section of the probe. One of these provides amplification and pulse shaping for the helium detector signals that are transmitted uphole in analog form. The second P.C. board contains the circuitry required to control the direction of travel of the gamma-ray source and to monitor the position of the source in the probe. Power supplies and a voltage regulator required for operating all downhole circuitry and for providing the bias to the helium proportional counter are located on the third P.C. board.

All power/electrical signals were transmitted over ~90 m (~300 ft) of 4 HO logging cable via the winch slip rings from/to the uphole electronics control module. This module serves as the control center for powering the probe electronics, controlling and monitoring the source position, and routing the helium detector signals from the slip rings to an Ortec 450 amplifier for further shaping and amplification. The output signals were sent to the ND660 computer-based multichannel analyzer where they were digitized and stored as pulse-height spectra. The spectra obtained were permanently recorded on floppy disk for further analysis on a nearly identical system at LASL.

D. Calibration Facility Data

The components of the photoneutron-based logging system were transported to the DOE uranium calibration facility in Grand Junction, Colorado, by LASL personnel in November 1979. The goals of the field trip were to determine the field-worthiness of the probe and to assess its response to uranium in a variety of borehole and formation conditions. As discussed previously, the first of these goals was clearly met. The second goal was also achieved as described below.

Static and dynamic data were obtained in the A and D models. The information gathered can be classified in three general categories, 1) calibration--tool response as a function of uranium ore grade with all other parameters fixed; 2) formation parameter effects--tool response as a function of formation density, porosity, and neutron-absorber content changes with ore grade fixed; and 3) borehole diameter calibration--tool response as a function of borehole diameter and fluid with all other parameters fixed.

1. Calibration. The calibration of the probe was determined by static measurements in models A1, A2, and A3, with both air and water as borehole fluids. Model A4 was also measured but the uranium concentration is not uniform with depth and the results were not used in establishing the calibration. Models A1 through A4 are each 1.83 m (6 ft) in diameter and 8.84 m (29 ft) deep with a vertical, 11.4-cm (4.5-in.) borehole in the center. There is a 1.52-m (5-ft)-thick barren zone at the top of each model, followed by a 1.83-m (6-ft) thick ore zone, and finally a 1.22-m (4-ft)-thick barren zone. The remaining 4.27 m (14 ft) at the bottom of the models contains a runout tube immediately below the borehole. The formation parameters for the ore zones of all models studied are given in Table I.

Careful static scans of models A3 and A4 were made with air as the borehole fluid, whereas a more limited number of data points were obtained in the ore zones and barren zones in the other cases. Table II details the calibration results both in terms of response per unit ore grade and response per unit U_3O_8 density. The weighted average response per unit U_3O_8 density is determined, at least in a relative sense, to better than ±2% for both water- and air-filled boreholes. These results are shown in the conventional way in Fig. 3.

TABLE I

FORMATION PARAMETERS FOR A AND D MODELS AT DOE GRAND JUNCTION CALIBRATION FACILITY

Model	Ore Grade ($ppm\ U_3O_8$)		Dry Bulk Density (g/cm^3)	Porosity (%)	Parameter
A-1	278	34	2.22	18 [a]	Ore-Grade
A-2	757	42	2.17	18 [a]	Ore-Grade
A-3	1550	81	2.18	18 [a]	Ore-Grade
A-4	2280 [b]	942	2.22	18 [a]	Ore-Grade
A-5-T	780	32	2.17	17.8	high Σ
A-5-B	824	91	2.40	17.8	high ρ
A-6-T	688	73	1.85	28.8	high ϕ
A-6-B	700 [b]	149	2.21	16.3	low ϕ
D	797	55	2.12	22.1 [a]	Borehole Diameter and Fluid

[a] Estimated

[b] Average values for nonuniform ore zone

TABLE II

PHOTONEUTRON-BASED LOGGING PROBE CALIBRATION DATA

A) Air-Filled

Model	Ore Grade (ppm U_3O_8)	Response[a] (cts/s)	Response/Ore Grade (cts/s-ppm U_3O_8 x 10^3)	Response[b]/U_3O_8 Density (cts/s-lb/ft^3 U_3O_8)
A-1	278	2.369 ± 0.047	8.52 ± 0.17[c]	61.5 ± 1.2 [c]
A-2	757	6.048 ± 0.227	7.99 ± 0.30	59.0 ± 2.2
A-3	1550	12.38 ± 0.31	7.99 ± 0.20	58.7 ± 1/5
		Weighted average:	8.25 ± 0.12	60.2 ± 0.9
		[d] χ^2/ν :	2.48	1.22

B) Water-Filled

A-1	278	1.028 ± 0.039	3.70 ± 0.14	26.7 ± 1.0
A-2	757	2.559 ± 0.040	3.38 ± 0.05	25.0 ± 0.4
A-3	1550	5.319 ± 0.153	3.43 ± 0.10	25.2 ± 0.7
		Weighted Average:	3.42 ± 0.04	25.2 ± 0.3
		[d] χ^2/ν :	2.26	1.28

[a] All data reported were obtained in the sidewalled configuration.

[b] Calculated from the ore grade by using the dry bulk density given in Table 1.

[c] The uncertainties in the response per unit ore grade and the response per unit U_3O_8 density have been calculated assuming no uncertainties in the ore grades and the dry bulk densities.

[d] The χ^2/ν values have been computed by assuming that the weighted average is the "best fit" value and has no uncertainty.

Including uncertainties for the model ore concentrations would yield response uncertainties far greater than the dispersion of the results warrants. The close agreement of the response values in Table II may be fortuitous, but this explanation seem unlikely in the case of four independent observations. Another possible explanation is that the estimated uncertainties in the ore grades given in Table I include systematic uncertainties, i.e., errors in scale. These, of course, would cancel in the analysis presented in Table II. Finally, it is possible that the stated uncertainties in ore grade for the models are indeed random but were measured over spatial intervals much smaller than the spatial resolution of the present tool. In this situation, the tool would average over many small measurement intervals with a subsequent reduction in the measurement variations as a function of depth.

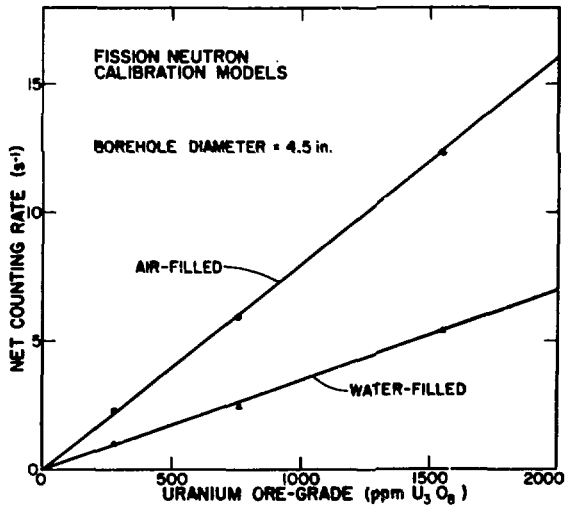

Fig. 3. Calibration data for the photoneutron-based uranium well-logging probe in Grand Junction models A-1, 2, and 3.

A dynamic scan of model A-3 (1550 ppm U_3O_8) was also performed. A precision of ±3% on the ore grade-thickness product was obtained at a logging speed of 0.5 cm/s (1 ft/min) with water as the borehole fluid. Data were dumped at 30-s intervals and a total of 12 minutes was required to define both the ore and barren zones. The precision of the ore grade-thickness product should scale as the square root of the logging speed, i.e., a precision of ±9% would be obtained at a logging speed of 5.1 cm/s (10 ft/min).

2. Formation Parameter Effects. Careful static scans of models A-5 and A-6 were performed to study the effects of variations in formation parameters on the performance of the tool. These models are similar to A-1 through A-4 except they are constructed with upper and lower ore zones 1.22 m (4 ft) thick and a middle barren zone 2.13 m (7 ft) thick. The parameters of interest are listed in Table I, while the data obtained are summarized in Table III.

TABLE III

FORMATION PARAMETER EFFECTS

A) Air-Filled

Model	Ore Grade (ppm U_3O_8)	Response (Cts/s)[a]	Response/U_3O_8 Density (Cts/s-lb/ft^3 U_3O_8)	Ratio Relative to A-2
A-5-T	780 ± 32	2.686 ± 0.109	25.4 ± 1.1	0.442 ± 0.019[b]
A-5-B	824 ± 91	2.512 ± 0.148	20.4 ± 1.2	0.339 ± 0.021
A-6-T	688 ± 73	9.235 ± 0.275	65.9 ± 3.5	1.09 ± 0.06
A-6-B	700 ±149	9.701 ± 0.219	59.1 ± 2.3	0.982 ± 0.041

B) Water-Filled

A-5-T	780 ± 32	1.088 ± 0.054	10.3 ± 0.5	0.409 ± 0.020
A-5-B	824 ± 91	0.922 ± 0.051	7.48 ± 0.41	0.297 ± 0.017
A-6-T	688 ± 73	2.149 ± 0.071	27.1 ± 0.9	1.08 ± 0.04
A-6-B	700 ±149	2.290 ± 0.073	23.7 ± 0.8	0.940 ± 0.034

[a] All data reported are in the sidewalled configuration.

[b] Uncertainties quoted in this column assume no uncertainty in the U_3O_8 concentration.

A-5-T(op) was designed to determine the effects on uranium ore-grade determination caused by variations in the thermal neutron absorption cross section in the formation. This model is similar to A-2 in all respects except for the thermal neutron absorption cross section, which has been increased by a factor of about four through the addition of B_4C. Referring to the last column of Table III, the effect of the additional thermal neutron absorption is to reduce the response of the probe to 40-45% of its calibrated response. This result is independent of borehole fluid. Since the low-energy portion of the ^{235}U fission cross section accounts for an important fraction of the number of fissions produced in the ore zone, a reduction in response of this order does not seem unreasonable considering the high thermal absorption cross section of boron.

A-5-B(ottom) was constructed using corundum rather than sand as the matrix material to assess the effects of increased bulk density on fission neutron tool response. For fixed ore grade, one expects the response of the tool to scale directly with density, if all other formation parameters also remain fixed. Instead, a reduction in response to 30-35% of the calibrated reponse is observed. This result is not understood at this time. There are, however, two possible explanations for the discrepancy. The first is that the uranium is simply not present in A-5-B in the quantity stated. Second, and more likely, is the presence of a high level of neutron poison.

A-6 was designed to determine the influence of changes in formation porosity on the response of fission neutron tools. As indicated in Table I, A-6-T and A-6-B have markedly different porosities and densities. Assuming that the effect on the response caused by the density difference can be properly corrected, a comparison of A-6-T and A-6-B will demonstrate the effects caused by porosity alone. Table III indicates a small increase in corrected tool response with increasing porosity for both the air- and water-filled cases. Crudely, for every one per cent increase (absolute) in the value of porosity, the response of the tool increases by one per cent (fractional) over this limited range of porosity values (16-29%). If this range is representative of "real" borehole conditions, porosity variations should not pose a significant problem for the photoneutron-based logging tool.

3. Borehole Diameter and Fluid Corrections. Corrections to tool response caused by variations in borehole diameter and fluid were determined in the D model. This model is 4.88 m (16 ft) in diameter by 8.84 m (29 ft) deep and contains seven boreholes ranging in diameter from 7.6 cm (3 in.) to 33 cm (13 in.). The boreholes were drilled in the pad at 2° with respect to vertical, ensuring that all reported measurements are in the side-walled configuration. There is a 1.52-m (5-ft)-thick barren zone at the top of the model, followed by a 1.83-m (6-ft)-thick ore zone and finally a 1.22-m (4-ft)-thick barren zone. The remaining 4.27 m (14 ft) at the bottom of the model accommodates run-out tubes at the bottom of each borehole. The formation parameters for the ore zone are given in Table I.

The response of the photoneutron-based probe to variations in borehole diameter and fluid are presented in Table IV and Fig. 4. For the air-filled case, the response is flat for diameters up to 22.9 cm (9 in.) but declines slowly for larger diameters. The water-filled borehole response is

TABLE IV

BOREHOLE DIAMETER AND
FLUID CALIBRATION (D MODEL)

Borehole Diameter (in)	Air-Filled Counting Rate	Water-Filled Counting Rate
4.50	5.37 ± 0.22	2.18 ± 0.10
6.00	5.54 ± 0.40	1.71 ± 0.18
7.56	5.44 ± 0.16	1.50 ± 0.07
9.00	5.36 ± 0.16	1.25 ± 0.06
11.00	4.71 ± 0.15	1.20 ± 0.07
13.00	4.30 ± 0.23	1.20 ± 0.06
Bkgd Counting Rates	0.727 ± 0.049	0.278 ± 0.026
Calibration Relative to A-1, 2, and 3 (4.50-in. diameter)	0.847 ± 0.039	0.821 ± 0.041

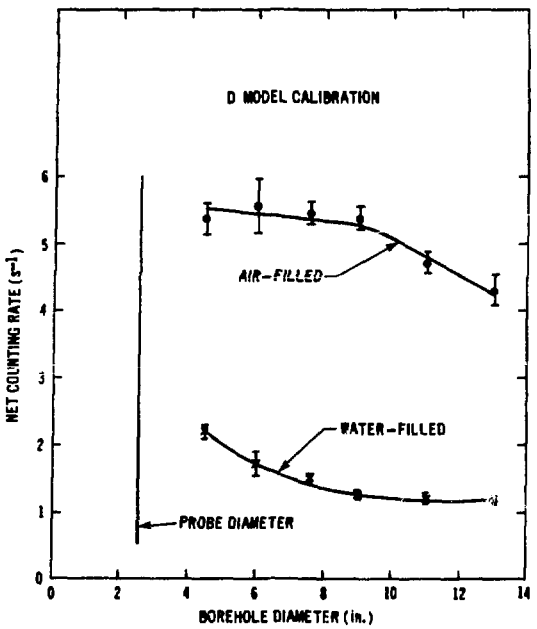

Fig. 4. Response of photoneutron-based uranium well-logging probe to variations in borehole diameter and fluid.

significantly lower than that of the air-filled case, as observed in the A models. The net counting rate falls with borehole diameter reaching an asymptotic value for diameters of 22.9 cm (9 in.) or more.

As indicated in Table IV, the presence of borehole fluid can readily be determined by observing the background counting rate in the barren formation. However, at this time, a method of independently deducing the borehole diameter has not been developed. Thus, the borehole diameter must be known as a function of depth to use the calibration curves shown in Fig. 4 to correct the uranium logging data.

The calibration of the D model, as determined in the 11.4-cm (4.5-in.)-diam borehole, is ∿15-20% lower than that obtained in the A models. Including the estimated effect of the porosity difference between the A and D models increases the discrepancy a few per cent more. It is not known at this time whether the disparity between the two model types is due to matrix effects or to a systematic difference in ore-grade assignment.

A dynamic scan of the 33-cm (13-in.) air-filled borehole of the D model was also performed. At a logging speed of 0.5 cm/s (1 ft/min), a precision of ∿± 4% was obtained for the ore-grade thickness product.

E. Conclusions

The major goals of the Grand Junction field trip have been achieved. The photoneutron-based well-logging probe has demonstrated adequate durability in the field and sufficient sensitivity to uranium to function at competitive logging speeds. The calibration of the probe is linear up to at least 2500 ppm U_3O_8 and has a sensitivity of about 80 (35) cts/s-% U_3O_8 for air (water)-filled, 11.4-cm (4.5-in.) boreholes. The detectability limit of the probe is ∿40 ppm (3σ) in 100 s of counting time. The probe response is reduced significantly by the presence of neutron poisons in the formation but has only a weak dependence on formation porosity. The major challenge remaining is to determine "self-contained" methods for quantifying the diameter of the borehole and formation neutron poison content.

ACKNOWLEDGMENTS

The authors appreciate the technical support received from the following Q-1 group members in the final testing of the photoneutron-based logging probe: R. Slice and K. Johnson, electronics; S. Beach and C. Spirio, coordination and planning; and L. G. Speir, mechanical testing.

REFERENCES

1. M. L. Evans, "NDA Technology for Uranium Resource Evaluation," Los Alamos Scientific Laboratory report LA-7617-PR (January 1979), pp. 24-32.

2. M. P. Baker, L. G. Speir, R. Slice, and G. Hackman, "NDA Technology for Uranium Resource Evaluation," Los Alamos Scientific Laboratory report LA-8321-PR (April 1980), pp. 8-15.